

**Nucleon strange  $s\bar{s}$  asymmetry to the  $\Lambda/\bar{\Lambda}$  fragmentation**Yujie Chi,<sup>1</sup> Xiaozhen Du,<sup>1</sup> and Bo-Qiang Ma<sup>1,2,3,\*</sup><sup>1</sup>*School of Physics and State Key Laboratory of Nuclear Physics and Technology, Peking University, Beijing 100871, China*<sup>2</sup>*Collaborative Innovation Center of Quantum Matter, Beijing, China*<sup>3</sup>*Center for High Energy Physics, Peking University, Beijing 100871, China*

(Received 7 July 2014; published 1 October 2014)

The difference between the  $\Lambda$  and  $\bar{\Lambda}$  longitudinal spin transfers in the semi-inclusive deep inelastic scattering process is intensively studied. The study is performed in the current fragmentation region, by considering the intermediate hyperon decay processes and sea quark fragmentation processes, while the strange sea  $s\bar{s}$  asymmetry in the nucleon is taken into account. The calculation in the light-cone quark-diquark model shows that the strange sea asymmetry gives a proper trend to the difference between the  $\Lambda$  and  $\bar{\Lambda}$  longitudinal spin transfers. When considering the nonzero final hadron transverse momentum, our results can explain the COMPASS data reasonably. The nonzero final hadron transverse momentum is interpreted as a natural constraint to the final hadron  $z$  range where the longitudinal spin transfer is more sensitive to the strange sea  $s\bar{s}$  asymmetry.

DOI: 10.1103/PhysRevD.90.074003

PACS numbers: 14.20.Jn, 13.60.Rj, 13.87.Fh, 13.88.+e

**I. INTRODUCTION**

The flavor structure of the nucleon sea, especially the existence of the strange sea  $s\bar{s}$  asymmetry, is of great importance in modern physics study. In earlier studies it is commonly assumed that the strange sea of the nucleon is particle-antiparticle  $s\bar{s}$  symmetric, but in fact this is manifested neither theoretically nor experimentally. In the basis of nonfundamental symmetry violation, much progress has been made in the study of the strange sea  $s\bar{s}$  asymmetry. We divide these studies into two groups. One is the study mainly focusing on the nonperturbative process that is believed to be able to produce an asymmetric intrinsic strange sea [1–18]. The other is the next-to-next-to-leading order perturbative evolution process which is pointed out to be able to cause an extrinsic strange sea asymmetry [18,19]. Studies from the nonperturbative aspect have suggested that the nuclear strange sea  $s\bar{s}$  asymmetry can give a possible explanation to the experimental CCFR data [20] and the NuTeV anomaly [21]. However, there is still no obvious evidence for the existence of the asymmetric strange nucleon sea.

The COMPASS collaboration measured the  $\Lambda$  and  $\bar{\Lambda}$  longitudinal spin transfers in the muon-nucleon semi-inclusive deep inelastic scattering (SIDIS) process [22]. Their measurement shows a quite different behavior for the  $\Lambda$  and  $\bar{\Lambda}$  on the  $x$  and  $x_F$  dependences of the longitudinal spin transfers. The spin transfer to  $\Lambda$  is small, compatible to zero, in the entire domain of the measured kinematic variables. In contrast, the longitudinal spin transfer to the  $\bar{\Lambda}$  increases with  $x_F$  reaching values of  $D_{LL}^{\bar{\Lambda}} = 0.4 \sim 0.5$ . It is pointed out in Ref. [15] that accurate measurement

of the spin transfers to the  $\Lambda$  and  $\bar{\Lambda}$  in the COMPASS kinematics has the potential to probe the intrinsic strangeness sea and their analysis mainly focuses on the target fragmentation contribution. The possibility of the strange-antistrange asymmetry contributing to the spin transfer difference of the  $\Lambda$  and  $\bar{\Lambda}$  is pointed out in Refs. [23,24], analyzed in the current fragmentation region.

In this paper, we provide a systematic study of the  $\Lambda$  and  $\bar{\Lambda}$  longitudinal spin transfer difference in the current fragmentation region, by considering the intermediate hyperon decay processes and sea quark fragmentation processes, while the strange sea  $s\bar{s}$  asymmetry of the nucleon is also taken into account in a reasonable way.

In Sec. II, we give the expression of the longitudinal spin transfer in a general  $\ell p \rightarrow \ell P_h X$  SIDIS process. Also, we calculate the valence quark distribution functions (PDFs) of octet baryons and the  $\Sigma^*$  hyperon in the light-cone quark-spectator-diquark model, as they are needed when we use the phenomenology Gribov-Lipatov relation to obtain the quark fragmentation functions (FFs). Considering the CTEQ5 parametrization [25] and the strange-antistrange asymmetry in the baryon-meson fluctuation model [1], we present our inputs of the nucleon FFs and PDFs in the longitudinal spin transfer calculation in Sec. III. In Sec. IV, we give our results and discussions using the exact relationship of  $x_F$  on the  $y$  and  $z$  kinematical variable dependences. We compare the calculated results with the COMPASS data. Our results indicate that the  $\Lambda$  and  $\bar{\Lambda}$  longitudinal spin transfer difference can be explained reasonably within the light-cone SU(6) quark-spectator-diquark model after considering the asymmetry between the  $s$  and  $\bar{s}$  quark distributions in the nucleon as well as the nonzero final hadron transverse momentum contribution. Finally, we give a short summary in Sec. V.

\*mabq@pku.edu.cn

## II. THE LONGITUDINAL SPIN TRANSFER AND THE LIGHT-CONE QUARK-SPECTATOR-DIQUARK MODEL

We start from the collinear factorization theorem in the SIDIS process. From the quantum chromodynamics (QCD) factorization theorem, the high energy collision cross section can be calculated by using the perturbation theory complemented with the soft QCD effects embedded in quark distributions and fragmentation functions, which are universal.

The differential scattering cross section at the tree level of a general  $\ell p \rightarrow \ell P_h X$  semi-inclusive deep inelastic scattering process can be expressed as [26]

$$\frac{d\sigma}{dx dy dz d^2\vec{P}_{h\perp}} = \frac{\pi\alpha_{\text{em}}^2 y}{2Q^4 z} L_{\mu\nu} W^{\mu\nu}, \quad (1)$$

where  $x = \frac{Q^2}{2P \cdot q}$ ,  $y = \frac{P \cdot q}{P \cdot \ell}$  and  $z = \frac{P \cdot P_h}{P \cdot q}$  are three Lorentz invariant variables,  $\vec{P}_{h\perp}$  is the transverse momentum of the produced hadron in the  $\gamma^* P$  collinear frame.  $L_{\mu\nu}$  and  $W^{\mu\nu}$  are leptonic and hadronic tensors respectively and their specific forms can be referred to Ref. [26].

Then in the parton model, for a longitudinally polarized charged lepton beam and an unpolarized target, if the produced hadron is polarized, the helicity asymmetry cross section is obtained as

$$A(x, y, z) = \frac{d\sigma_{\uparrow} - d\sigma_{\downarrow}}{d\sigma_{\uparrow} + d\sigma_{\downarrow}} = \frac{\frac{4\pi\alpha_{\text{em}}^2 S}{Q^4} \sum_a e_a^2 xy(1-y/2) f_a(x, Q^2) \Delta D_a(z, Q^2)}{\frac{4\pi\alpha_{\text{em}}^2 S}{Q^4} \sum_a e_a^2 x \frac{1+(1-y)^2}{2} f_a(x, Q^2) D_a(z, Q^2)}, \quad (2)$$

where the subscript  $\uparrow$  or  $\downarrow$  denotes the helicity of the produced baryon being parallel or antiparallel to the helicity of the initial incident beam,  $e_a$  is the electric charge of  $a$ ,  $f_a(x, Q^2)$  is the unpolarized parton distribution function, and  $D_a(z, Q^2)$ ,  $\Delta D_a(z, Q^2)$  are the unpolarized and polarized fragmentation functions respectively, with  $a$  representing the quark or antiquark flavors,  $-Q^2 = -Sxy$  being the squared 4-momentum transfer of the virtual photon, and  $S = M_p^2 + m_\ell^2 + 2M_p E_\ell$  being the squared energy in the lepton-proton center-of-mass frame.

For a longitudinally polarized charged lepton beam and an unpolarized target, if the longitudinal polarization of the incoming lepton beam is  $P_B$ , the struck quark acquires a polarization  $P_q = P_B D(y)$  directed along its momentum. The  $D(y)$ , whose explicit expression is

$$D(y) = \frac{1 - (1-y)^2}{1 + (1-y)^2}, \quad (3)$$

is the longitudinal depolarization factor taking into account the loss of polarization of the virtual photon as compared to that of the lepton. The  $P_B D(y)$  distribution can be determined by subtraction of the averaged distribution of the sideband events from the distribution of the events in the signal region according to the COMPASS experiment [22]. The spin transfer describes the probability that the polarization of the struck quark along the primary quantization axis  $L$  is transferred to the  $\Lambda$  hyperon along the secondary quantization axis  $L'$ . The longitudinal spin transfer relates the produced  $\Lambda$  polarization  $P'_L$  to the polarization of incoming lepton beam  $P_B$  by [27]

$$P'_L = P_B D(y) A_{LL'}^\Lambda, \quad (4)$$

where  $A_{LL'}^\Lambda$  is the longitudinal spin transfer. In the COMPASS experiment, both the  $L$  and  $L'$  are chosen along the virtual photon momentum [22], thus we can omit the subscripts.

In this paper, we preserve all the variables appearing in Eq. (2), trying to give a proper longitudinal spin transfer form. After removing the depolarization factor  $D(y)$  from the asymmetry cross section, the longitudinal spin transfer is obtained as

$$A(x, z) = \frac{\int dy \frac{Sx}{Q^4} \sum_a e_a^2 f_a(x, Q^2) \Delta D_a(z, Q^2)}{\int dy \frac{Sx}{Q^4} \sum_a e_a^2 f_a(x, Q^2) D_a(z, Q^2)}. \quad (5)$$

After integrating the numerator and denominator on  $y$  and  $x$  (or  $z$ ) sequentially, we can obtain the longitudinal spin transfer on various kinematical variables.

When we discuss the contributions of  $\Lambda$  hyperons produced from the intermediate heavier hyperon decays in the SIDIS process, it is common to think that the struck quark first fragments to various hadrons, and then some hadrons decay to  $\Lambda$  according to the branching ratios that the intermediate hyperons decay to  $\Lambda$ . The probabilities that the struck quark fragments to various hadrons ( $\Lambda$ ,  $\Sigma^0$ ,  $\Sigma^*$ , etc.) are different considering the mass difference of these hadrons, and this effect should be taken into account when we calculate the contributions of the intermediate heavier hyperon decaying process according to their branching ratios. However, the probabilities that the struck quark fragments to various hadrons in the  $\Lambda$  production process are unknown to us.

In our calculation, the normalization of the fragmentation functions used in Eq. (5) is chosen as  $\int dz D_a^h(z)/z = 1$  for each hadron  $h$ , for the convenience to use the relation between the fragmentation functions and distribution functions in our discussion later. However, the real defined fragmentation functions  $D_a^h(z)$  are normalized as  $\sum_h \int dz z D_a^h(z) = 1$ . Considering this difference between these two normalizations of the fragmentation functions, there should be factors in front of the fragmentation functions we used to reflect the probabilities that the quark

fragments to various hadrons. We notice that this factor in front of the total quark to  $\Lambda$  fragmentation function makes no difference to our calculation since fragmentation functions appear both in the numerator and denominator in Eq. (5).

The Monte Carlo calculation is used to obtain the ratios of the final  $\Lambda$  hyperons produced from different channels including the direct quark fragmentation process and the intermediate hyperon decaying process. Because the probabilities that the struck quark fragments to various hadrons are already included in these ratios, it is feasible to multiplying these ratios to our calculated fragmentation functions.

A Monte Carlo calculation using the LEPTO generator indicates that only about 40%–50% of  $\Lambda$ 's are produced directly, 30%–40% originate from  $\Sigma^*(1385)$  decay and about 20% are decay products of the  $\Sigma^0$ . The COMPASS collaboration measured the relative weights of the  $\Sigma^*$  and the  $\Xi$  hyperon decaying to the  $\Lambda\pi$ . The results are about 20% smaller than those of the Monte Carlo calculation [28].

For the semi-inclusive  $\mu p \rightarrow \mu\Lambda X$  process, when the intermediate decay process effects are considered, the helicity-dependent fragmentation function  $\Delta D^a(z, Q^2)$  and the unpolarized fragmentation function  $D^a(z, Q^2)$  of the  $\Lambda$  hyperon can be reasonably written as

$$\begin{aligned} \Delta D_{\Lambda}^q(z, Q^2) &= a_1 \Delta D_{q\Lambda}(z, Q^2) + a_2 \Delta D_{\Sigma^0}^q(z', Q^2) \alpha_{\Sigma^0\Lambda} \\ &\quad + a_3 \Delta D_{\Sigma^*}^q(z', Q^2) \alpha_{\Sigma^*\Lambda} \\ &\quad + a_4 \Delta D_{\Xi}^q(z', Q^2) \alpha_{\Xi\Lambda}, \end{aligned} \quad (6)$$

and

$$\begin{aligned} D_{\Lambda}^{q(\bar{q})}(z, Q^2) &= a_1 D_{q(\bar{q})\Lambda}(z, Q^2) + a_2 D_{\Sigma^0}^{q(\bar{q})}(z', Q^2) \\ &\quad + a_3 D_{\Sigma^*}^{q(\bar{q})}(z', Q^2) + a_4 D_{\Xi}^{q(\bar{q})}(z', Q^2), \end{aligned} \quad (7)$$

where  $\bar{q}$  flavors are assumed to be unpolarized in this process.

As for the  $\mu p \rightarrow \mu\bar{\Lambda} X$ , we just change the particles into their antiparticles in Eqs. (6) and (7), and the same consideration should be kept in the following discussions.

The  $a$ 's are weight coefficients which indicate the ratios of contribution from different decay channels. Their values are adjusted as

$$a_1 = 0.4, \quad a_2 = 0.2, \quad a_3 = 0.3, \quad a_4 = 0.1, \quad (8)$$

based on the spirit of the Monte Carlo predictions [26].

In the specific calculation, the weight coefficients of the  $\Sigma^*$  hyperon are divided by three types of particles, that are  $\Sigma^+(1385)$ ,  $\Sigma^0(1385)$  and  $\Sigma^-(1385)$ , while each type has two positively polarized spin states, i.e.,  $(3/2, 3/2)$  and  $(3/2, 1/2)$ . So the contribution to the spin transfer from the  $\Sigma^*$  is actually a mixture. To simplify this issue, we take 10% for each branch as an average. The same treatment is done

to the  $\Xi$  hyperon, which contains the contribution from the  $\Xi^0$  and  $\Xi^-$ , and 5% is given to each branch.

The  $\alpha$ 's are decay parameters, representing the polarization transfer from the decay hyperons to the  $\Lambda$ . In our study, these parameters are set as

$$\begin{aligned} \alpha_{\Sigma^0\Lambda} &= -0.333, & \alpha_{\Sigma^*(\frac{3}{2}, \frac{3}{2})\Lambda} &= 1.0, \\ \alpha_{\Sigma^*(\frac{3}{2}, \frac{1}{2})\Lambda} &= 0.333, & \alpha_{\Xi^0\Lambda} &= -0.406, \\ \alpha_{\Xi^-\Lambda} &= -0.458. \end{aligned} \quad (9)$$

The values of  $\alpha_{\Sigma^0\Lambda}$ ,  $\alpha_{\Xi^0\Lambda}$  and  $\alpha_{\Xi^-\Lambda}$  are taken from Refs. [29,30], while  $\alpha_{\Sigma^*\Lambda}$ 's are estimated parameters by us. The decay parameters of  $\Sigma^*$  are given separately for the two types of the positive spin states. The choice of an  $\alpha_{\Sigma^*(\frac{3}{2}, \frac{3}{2})\Lambda} = 1.0$  is due to the facts that the spin of  $\Sigma^*$  (being  $3/2$ ) should be almost total positively correlated with  $\Lambda$  spin (being  $1/2$ ) in the decay process corresponding to the  $(s, s_z) = (3/2, 3/2)$  components, and the choice of an  $\alpha_{\Sigma^*(\frac{3}{2}, \frac{1}{2})\Lambda} = 0.333$  is the calculated result from the  $(s, s_z) = (3/2, 1/2)$  components in the decay mode  $\Sigma^* \rightarrow \Lambda\pi$ , according to the angular-momentum conservation law. In the decay model  $\Sigma^* \rightarrow \Lambda\pi$ , if the spin angular momentum of  $\Sigma^*$  is  $(s, s_z) = (3/2, 1/2)$ , and the spin angular momentums of  $\Lambda$  and  $\pi$  are  $(s, s_z) = (1/2, \pm 1/2)$  and  $(s, s_z) = (0, 0)$  respectively, the orbital angular momentum between  $\Lambda$  and  $\pi$  is  $(L, L_z) = (1, \pm 1)$  or  $(L, L_z) = (1, 0)$ . To obtain the  $(s, s_z) = (3/2, 1/2)$  component of  $\Sigma^*$ , we should take  $(L, L_z) = (1, 1)$  or  $(L, L_z) = (1, 0)$ . From the Clebsch-Gordan coefficients, we know that the probability of the production of the  $(s, s_z) = (1/2, 1/2)$  component of  $\Lambda$  is  $2/3$ , and that the probability of the production of the  $(s, s_z) = (1/2, -1/2)$  component of  $\Lambda$  is  $1/3$ . Thus we get  $\alpha_{\Sigma^*(\frac{3}{2}, \frac{1}{2})\Lambda} = 0.333$ .

In the intermediate decay process, i.e.,  $q \rightarrow H_i \rightarrow \Lambda$ , the longitudinal momentum fraction of the  $\Lambda$  hyperon to the splitting quark  $q$  should be less than that of the decay hyperon  $H_i$  to  $q$ . This can be inferred from the momentum fraction  $z$  definition in the light-cone formalism,  $z = \frac{P_{\Lambda}^-}{q^-}$ , for the final detected  $\Lambda$  hyperon. This effect is taken into account by redefining  $\frac{P_{\Lambda}^-}{q^-} = 1.1 * \frac{P_{H_i}^-}{q^-}$ , i.e.,  $z' = 1.1 * z$ . The relation  $z' = 1.1z$  we used is a very rough estimate based on the energy-momentum conservation law and the mass relation of the particles appearing in the intermediate hyperon decay process.

We then consider the Melosh-Wigner rotation effect in the calculation of the parton densities [31–33], and apply the valence quark distribution functions calculated in the light-cone SU(6) quark-spectator-diquark model [34] to estimate the probability of a valence quark directly fragmenting to a hadron. This can be realized through the phenomenology Gribov-Lipatov relation [35–38],

$$D_q^h(z) \sim zq_h(z), \quad (10)$$

where the fragmentation function  $D_q^h(z)$  indicates a quark  $q$  splitting into a hadron  $h$  with longitudinal momentum fraction  $z$ , and the distribution function  $q_h(z)$  presents the probability of finding the same quark  $q$  carrying longitudinal momentum fraction  $x = z$  inside the same hadron  $h$ . Although the Gribov-Lipatov relation is only known to be valid near the  $z \rightarrow 1$  and on a certain energy scale  $Q_0^2$  in the leading order approximation, it is interesting to note that such a relation provides successful descriptions of the available  $\Lambda$  polarization data in several processes [9,24,39], based on quark distribution of the  $\Lambda$  in the quark-diquark model and in the pQCD based counting rule analysis. Thus we can consider Eq. (10) as a phenomenological ansatz to parametrize the quark to  $\Lambda$  fragmentation functions, and then check the validity and reasonableness of this method by comparing the theoretical predictions with the experimental observations.

The main idea of the light-cone SU(6) quark-spectator-diquark model is to start from the naive SU(6) wave function of the hadron and then if any one of the quarks is probed, reorganize the other two quarks in terms of two quark wave functions with spins 0 or 1 (scalar and vector diquarks), i.e., the diquark serves as an effective particle which is called the spectator.

The unpolarized quark distribution for a quark with flavor  $q$  inside a hadron  $h$  is expressed as

$$q(x) = c_q^S a_S(x) + c_q^V a_V(x), \quad (11)$$

where  $c_q^S$  and  $c_q^V$  are the weight coefficients determined by the SU(6) wave function, and  $a_D(x)$  ( $D = S$  for scalar spectator or  $V$  for axial vector spectator) denotes the amplitude for quark  $q$  to be scattered while the spectator is in the diquark state  $D$ , when expressed in terms of the light-cone momentum space wave function  $\varphi(x, \mathbf{k}_\perp)$ , reads

$$a_D(x) \propto \int [d^2\mathbf{k}_\perp] |\varphi(x, \mathbf{k}_\perp)|^2 \quad (D = S \text{ or } V), \quad (12)$$

and the normalization satisfies  $\int_0^1 dx a_D(x) = 3$ . To obtain a practical formalism of  $a_D(x)$ , the Brodsky-Huang-Lepage prescription [40] of the light-cone momentum space wave function for the quark-diquark is employed:

$$\varphi(x, \mathbf{k}_\perp) = A_D \exp \left\{ -\frac{1}{8\alpha_D^2} \left[ \frac{m_q^2 + \mathbf{k}_\perp^2}{x} + \frac{m_D^2 + \mathbf{k}_\perp^2}{1-x} \right] \right\}, \quad (13)$$

with the parameter  $\alpha_D = 330$  MeV. Other parameters in this model such as the quark mass  $m_q$ , vector (scalar) diquark mass  $m_D$  ( $D = S, V$ ) for the octet baryons are just simply estimated from the masses of the baryons. For  $u$  and  $d$  quarks, we take  $m_q \sim m_N/3$ . The masses of the scalar and vector diquarks should be different taking into account the spin force from color magnetism or alternatively from instantons [41]. QCD color-magnetic effects lift the mass degeneracy between hadrons that differ only in the orientation of quark spins, such as  $N$  and  $\Delta$ . The interaction is repulsive if the spins are parallel, so that a pair of quarks in

TABLE I. The quark distribution functions of octet baryons in the light-cone SU(6) quark-diquark model [39].

Baryon	$q$	$\Delta q$	$m_q$ (MeV)	$m_V$ (MeV)	$m_S$ (MeV)		
p	$u$	$\frac{1}{6}a_V + \frac{1}{2}a_S$	$\Delta u$	$-\frac{1}{18}\tilde{a}_V + \frac{1}{2}\tilde{a}_S$	330	800	600
(uud)	$d$	$\frac{1}{3}a_V$	$\Delta d$	$-\frac{1}{9}\tilde{a}_V$	330	800	600
n	$u$	$\frac{1}{3}a_V$	$\Delta u$	$-\frac{1}{9}\tilde{a}_V$	330	800	600
(udd)	$d$	$\frac{1}{6}a_V + \frac{1}{2}a_S$	$\Delta d$	$-\frac{1}{18}\tilde{a}_V + \frac{1}{2}\tilde{a}_S$	330	800	600
$\Sigma^+$	$u$	$\frac{1}{6}a_V + \frac{1}{2}a_S$	$\Delta u$	$-\frac{1}{18}\tilde{a}_V + \frac{1}{2}\tilde{a}_S$	330	950	750
(uus)	$s$	$\frac{1}{3}a_V$	$\Delta s$	$-\frac{1}{9}\tilde{a}_V$	480	800	600
$\Sigma^0$	$u$	$\frac{1}{12}a_V + \frac{1}{4}a_S$	$\Delta u$	$-\frac{1}{36}\tilde{a}_V + \frac{1}{4}\tilde{a}_S$	330	950	750
(uds)	$d$	$\frac{1}{12}a_V + \frac{1}{4}a_S$	$\Delta d$	$-\frac{1}{36}\tilde{a}_V + \frac{1}{4}\tilde{a}_S$	330	950	750
	$s$	$\frac{1}{3}a_V$	$\Delta s$	$-\frac{1}{9}\tilde{a}_V$	480	800	600
$\Sigma^-$	$d$	$\frac{1}{6}a_V + \frac{1}{2}a_S$	$\Delta d$	$-\frac{1}{18}\tilde{a}_V + \frac{1}{2}\tilde{a}_S$	330	950	750
(dds)	$s$	$\frac{1}{3}a_V$	$\Delta s$	$-\frac{1}{9}\tilde{a}_V$	480	800	600
$\Lambda^0$	$u$	$\frac{1}{4}a_V + \frac{1}{12}a_S$	$\Delta u$	$-\frac{1}{12}\tilde{a}_V + \frac{1}{12}\tilde{a}_S$	330	950	750
(uds)	$d$	$\frac{1}{4}a_V + \frac{1}{12}a_S$	$\Delta d$	$-\frac{1}{12}\tilde{a}_V + \frac{1}{12}\tilde{a}_S$	330	950	750
	$s$	$\frac{1}{3}a_S$	$\Delta s$	$\frac{1}{3}\tilde{a}_S$	480	800	600
$\Xi^-$	$d$	$\frac{1}{3}a_V$	$\Delta d$	$-\frac{1}{9}\tilde{a}_V$	330	1100	900
(dss)	$s$	$\frac{1}{6}a_V + \frac{1}{2}a_S$	$\Delta s$	$-\frac{1}{18}\tilde{a}_V + \frac{1}{2}\tilde{a}_S$	480	950	750
$\Xi^0$	$u$	$\frac{1}{3}a_V$	$\Delta u$	$-\frac{1}{9}\tilde{a}_V$	330	1100	900
(uss)	$s$	$\frac{1}{6}a_V + \frac{1}{2}a_S$	$\Delta s$	$-\frac{1}{18}\tilde{a}_V + \frac{1}{2}\tilde{a}_S$	480	950	750



a spin-1 state (vector) has higher energy than a pair of quarks in a spin-0 state (scalar). The energy shift between scalar and vector diquarks produces the  $N$ - $\Delta$  mass splitting. We take  $m_S = 600$  MeV and  $m_V = 800$  MeV for the scalar and vector diquarks to explain the  $N$ - $\Delta$  mass different [42]. To obtain the mass of scalar and vector diquarks containing one strange quark, we use the phenomenological fact that the strange quark adds about 150 MeV. Thus we get  $m_S = 750$  MeV and  $m_V = 950$  MeV for scalar and vector diquarks containing one strange quark;  $m_S = 900$  MeV and  $m_V = 1100$  MeV for scalar and vector diquarks containing two strange quarks. The free parameters are reduced to only a few numbers, which can be referred to in Table I.

The polarized quark distributions are obtained by introducing the Melosh-Wigner correction factor [32,33],

$$\Delta q(x) = \tilde{c}_q^S \tilde{a}_S(x) + \tilde{c}_q^V \tilde{a}_V(x), \quad (14)$$

where the coefficients  $\tilde{c}_q^S$  and  $\tilde{c}_q^V$  are also determined by the SU(6) quark-diquark wave function, and  $\tilde{a}_D(x)$  is expressed as

$$\tilde{a}_D(x) = \int [d^2\mathbf{k}_\perp] W_D(x, \mathbf{k}_\perp) |\varphi(x, \mathbf{k}_\perp)|^2 \quad (D = S \text{ or } V), \quad (15)$$

where

$$W_D(x, \mathbf{k}_\perp) = \frac{(k^+ + m_q)^2 - \mathbf{k}_\perp^2}{(k^+ + m_q)^2 + \mathbf{k}_\perp^2}, \quad (16)$$

with  $k^+ = x\mathcal{M}$  and  $\mathcal{M}^2 = \frac{m_q^2 + \mathbf{k}_\perp^2}{x} + \frac{m_D^2 + \mathbf{k}_\perp^2}{1-x}$ . The weight coefficients are also listed in Table I. In this model, though the mass difference between different quarks and diquarks breaks the SU(3) symmetry explicitly, the SU(3) symmetry between the octet baryons is in principle maintained in formalism.

Based on the same consideration, we give the distribution functions for the  $\Sigma^*$  hyperon, which in the naive quark

model is a member of the SU(3) decuplet with the total spin of 3/2. Here, we try to use the same parameters to estimate both the helicity and quark distribution functions in the light-cone SU(6) quark-spectator-diquark model based on the following reasons: (1) the mass of  $\Sigma^*$  (which is about 1385 MeV) is similar to that of  $\Xi^-$  (which is about 1321 MeV), so we can use the same effective quark mass parameters; (2) the total quark orbital angular momentum of  $\Sigma^*$  is 0, so to form a spin 3/2 particle, the diquark can only be in the vector state. The specific helicity-dependent and unpolarized quark distribution functions for the  $\Sigma^*$ 's in the quark-spectator-diquark model are shown in Table II.

### III. THE INPUTS OF THE NUCLEON FFs AND PDFs IN THE LONGITUDINAL SPIN TRANSFER CALCULATIONS

We know that in the naive quark model, there is an SU(3) flavor symmetry relation between octet baryons. We consider the antiquark distribution inside the octet baryons in the same way. To compare with the experimental data, the CTEQ5 parametrization (ctq5l) for proton [25] is used as an input:

$$\begin{aligned} u_v^p(x) &= u_v^{\text{ctq}}(x), \\ d_v^\Lambda(x) &= u_v^\Lambda(x) = \frac{u_v^{\Lambda, \text{th}}(x)}{u_v^{p, \text{th}}(x)} * u_v^{\text{ctq}}(x), \\ s_v^\Lambda(x) &= \frac{s_v^{\Lambda, \text{th}}(x)}{u_v^{p, \text{th}}(x)} * u_v^{\text{ctq}}(x), \\ \Delta d_v^\Lambda(x) &= \Delta u_v^\Lambda(x) = \frac{\Delta u_v^{\Lambda, \text{th}}(x)}{u_v^{p, \text{th}}(x)} * u_v^{\text{ctq}}(x), \\ \Delta s_v^\Lambda(x) &= \frac{\Delta s_v^{\Lambda, \text{th}}(x)}{u_v^{p, \text{th}}(x)} * u_v^{\text{ctq}}(x), \\ d_s^\Lambda(x) &= u_s^\Lambda(x) = \bar{u}^\Lambda(x) = \frac{1}{2} (\bar{u}^{\text{ctq}}(x) + \bar{d}^{\text{ctq}}(x)), \\ s_s^\Lambda(x) &= \bar{s}^\Lambda(x) = \bar{d}^{\text{ctq}}(x), \end{aligned} \quad (17)$$

TABLE II. The quark distribution functions of  $\Sigma(1385)$ 's in the light-cone SU(6) quark-diquark model.

Baryon	$q$	$\Delta q$	(3/2, 3/2)	(3/2, 1/2)	$m_q$ (MeV)	$m_V$ (MeV)
$\Sigma^+(1385)$	$u$	$\frac{2}{3}a_V$	$\frac{2}{3}\tilde{a}_V$	$\frac{2}{9}\tilde{a}_V$	330	950
(uus)	$s$	$\frac{1}{3}a_V$	$\frac{1}{3}\tilde{a}_V$	$\frac{1}{9}\tilde{a}_V$	480	800
$\Sigma^0(1385)$	$u$	$\frac{1}{3}a_V$	$\frac{1}{3}\tilde{a}_V$	$\frac{1}{9}\tilde{a}_V$	330	950
(uds)	$d$	$\frac{1}{3}a_V$	$\frac{1}{3}\tilde{a}_V$	$\frac{1}{9}\tilde{a}_V$	330	950
	$s$	$\frac{1}{3}a_V$	$\frac{1}{3}\tilde{a}_V$	$\frac{1}{9}\tilde{a}_V$	480	800
$\Sigma^-(1385)$	$d$	$\frac{2}{3}a_V$	$\frac{2}{3}\tilde{a}_V$	$\frac{1}{9}\tilde{a}_V$	330	950
(dds)	$s$	$\frac{1}{3}a_V$	$\frac{1}{3}\tilde{a}_V$	$\frac{1}{9}\tilde{a}_V$	480	800

where the  $u_v^{\text{ctq}}(x)$  means the PDF for the valence  $u$  quark inside the proton from the CTEQ5L parametrization, and the  $u_v^{\Lambda, \text{th}}(x)$  is the PDF for the valence  $u$  quark inside the  $\Lambda$  given by the light-cone SU(6) quark-diquark model, so as for the other flavors. For the other hyperons, the same spirit is followed. Applying the Gribov-Lipatov relation again, we can obtain the antiquark FFs to the same hyperon.

So far, we have given all the FFs used in the calculation. In the following, we discuss the input of the nucleon PDFs in the longitudinal spin transfer calculations.

In the baryon-meson fluctuation model [1], the nucleon wave function is considered to be a fluctuating system coupling to intermediate hadronic Fock states such as noninteracting meson-baryon pairs and the coupling that the proton to the virtual  $K^+\Lambda$  state is figured out to be of most importance in the production of the intrinsic strange and antistrange asymmetric sea. In this picture, the momentum distribution of the intrinsic  $s$  and  $\bar{s}$  quarks can be modeled in a two-level convolution formula:

$$\begin{aligned} s^{\text{th}}(x) &= \int_x^1 \frac{dy}{y} f_{\Lambda/K^+\Lambda}(y) q_{s/\Lambda}\left(\frac{x}{y}\right), \\ \bar{s}^{\text{th}}(x) &= \int_x^1 \frac{dy}{y} f_{K^+/K^+\Lambda}(y) q_{\bar{s}/K^+}\left(\frac{x}{y}\right), \end{aligned} \quad (18)$$

where  $f_{\Lambda/K^+\Lambda}(y)$ ,  $f_{K^+/K^+\Lambda}(y)$  are probabilities to find  $\Lambda, K^+$  in the  $K^+\Lambda$  state with longitudinal momentum fraction  $y$ ,  $q_{s/\Lambda}(\frac{x}{y})$ ,  $q_{\bar{s}/K^+}(\frac{x}{y})$  are probabilities to find  $q, \bar{q}$  in the  $\Lambda, K^+$  states with longitudinal momentum fraction  $\frac{x}{y}$  and these quantities can be calculated by adopting the two-body wave functions for  $p = K^+\Lambda$ ,  $K^+ = u\bar{s}$ ,  $\Lambda = s(ud)$ . The Gaussian-type two-body wave function is

$$\psi_{\text{Gaussian}}(M^2) = A_{\text{Gaussian}} \exp\left(-\frac{M^2}{8\alpha^2}\right), \quad (19)$$

where  $M^2 = \sum_{i=1}^2 (\mathbf{k}_{\perp i}^2 + m_i^2)/x_i$  is the invariant mass of the  $K^+\Lambda$ ,  $u\bar{s}$  or  $s(ud)$  two-body states, and  $\alpha = 330$  MeV is the scaling parameter.

As is pointed out, the fluctuation model can give the intrinsic strange sea asymmetry, which can partly explain some important experimental phenomena, such as the strange magnetic momentum and the NuTeV anomaly etc. [5,6,9,10,13]. However, its predictions do not take into account QCD evolution effects. We also know that the CTEQ5L parametrization for the  $s$  and  $\bar{s}$  are flavor blind and the result is in fact an average. In our study, we keep the asymmetry property given by the fluctuation model while in order to reflect the evolution effects a reasonable form of the nucleon strange sea input is given as

$$\begin{aligned} s^p(x) &= \frac{2s^{\text{th}}(x)}{s^{\text{th}}(x) + \bar{s}^{\text{th}}(x)} s^{\text{ctq}}(x), \\ \bar{s}^p(x) &= \frac{2\bar{s}^{\text{th}}(x)}{s^{\text{th}}(x) + \bar{s}^{\text{th}}(x)} s^{\text{ctq}}(x). \end{aligned} \quad (20)$$

As for other flavors, such as  $u, d, \bar{u}$  etc., the inputs are directly from the CTEQ5L parametrization.

#### IV. RESULTS AND DISCUSSION

We examine the longitudinal spin transfer on the  $x$  and the Feynman  $x_F$  variable dependences. The calculation of the  $x_F$  dependent spin transfer in our formula should be done through a kinematical transformation to relate to the  $x$ ,  $y$  and  $z$  variables.

We give the exact relationship as (see the Appendix)

$$\begin{aligned} x_F &= \frac{Syz}{M[M^2 + Sy(1-x)]} \left[ \left( M + \frac{Sy}{2M} \right) \right. \\ &\quad \left. \times \sqrt{\frac{1 - [4M^2(M_h^2 + P_{h\perp}^2)]}{(Syz)^2}} - \sqrt{\frac{S^2y^2}{4M^2} + Sxy} \right]. \end{aligned} \quad (21)$$

As is known, the factorization of the scattering cross section in our discussion is given in an ideal condition, that is  $Q^2 \rightarrow \infty$ ,  $P_{h\perp} \propto \mathcal{O}_M$ . In this condition, the  $P_{h\perp}$  can be neglected in Eq. (A6). However, the experimental data are in fact experimental condition affected, so our calculation should not be performed in an ideal way. We try to give some nonzero value for the  $P_{h\perp}$  valuable (several GeV, of order  $M$ ) and find that the nonzero input of the  $P_{h\perp}$  may affect the constraints between the  $x_F$ ,  $x$ ,  $y$  and  $z$  kinematical variables. The contour plots of these variables are given in Fig. 1 in the COMPASS experiment condition, where  $S = 320$  GeV<sup>2</sup>. We can see from the figures that with the increase of the  $P_{h\perp}$ , and the increase of the  $x$  variable, at the same  $x_F$  numerical point, the region of the  $z$  variable is significantly right shifted.

We then discuss the longitudinal spin transfer difference given by the COMPASS collaboration in two steps. In the first step, we first set  $P_{h\perp} = 0$  and consider the influence from the nucleon asymmetric strange sea input, then on the asymmetric strange sea input basis, we give two nonzero values to the  $P_{h\perp}$  variable. In the second step, we set the nucleon strange sea symmetric and see the influence from the nonzero  $P_{h\perp}$  variable. All these discussions are performed under the COMPASS experimental cuts  $1 \text{ GeV}^2 < Q^2 < 50 \text{ GeV}^2$ ,  $0.005 < x < 0.65$ ,  $0.2 < y < 0.9$ ,  $0.05 < x_F < 0.5$  and by the integration of equations

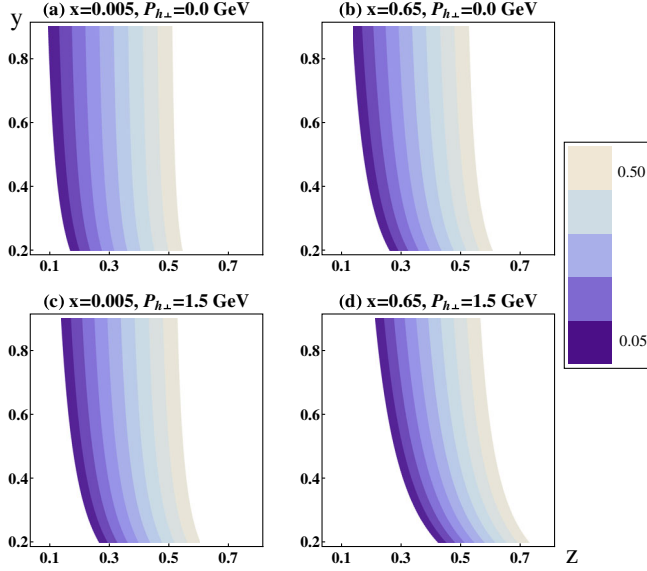


FIG. 1 (color online). The results of the  $x_F$  on the  $y$  and  $z$  kinematical variable dependences. The plot region of the  $x_F$  variable is 0.05  $\sim$  0.50. The subfigures are a series of results with different  $x$  and  $P_{h\perp}$  values.

$$A_\Lambda(x) = \frac{\int dy dz \frac{S_x}{Q^4} \sum_q e_q^2 f_q(x, Q^2) \Delta D_\Lambda^q(z, Q^2)}{\int dy dz \frac{S_x}{Q^4} \sum_q [e_q^2 f_q(x, Q^2) D_\Lambda^q(z, Q^2) + (q \rightarrow \bar{q})]}, \quad (22)$$

and

$$A_{\bar{\Lambda}}(x) = \frac{\int dy dz \frac{S_x}{Q^4} \sum_{\bar{q}} e_{\bar{q}}^2 f_{\bar{q}}(x, Q^2) \Delta D_{\bar{\Lambda}}^{\bar{q}}(z, Q^2)}{\int dy dz \frac{S_x}{Q^4} \sum_q [e_q^2 f_q(x, Q^2) D_{\bar{\Lambda}}^q(z, Q^2) + (q \rightarrow \bar{q})]}. \quad (23)$$

Equations (6) to (10), (17) to (20) as well as Tables I and II are all used to do the specific integrations.

The integration results are shown in Figs. 2, 3, 4 and 5. Among which, Figs. 2 and 3 are the first step calculation results of the  $x$  and  $x_F$  variable dependences. Figure 2(a) shows the result from the integration without considering the asymmetric sea effect or the nonzero  $P_{h\perp}$  effect, while in Fig. 2(b), the asymmetric sea effect expressed in Eq. (20) is taken into account. Figures 2(c) and 2(d) are results by considering both the asymmetric sea effect and the nonzero  $P_{h\perp}$  effect. As is shown, the input of the asymmetric sea effect gives more proper trend to the spin transfer difference than the pure integration one. Then after considering nonzero  $P_{h\perp}$  values, the difference between the spin transfers of  $\Lambda$  and  $\bar{\Lambda}$  get enlarged with an increasing  $P_{h\perp}$ . At the condition of  $P_{h\perp} = 3.0$  GeV, the result we get is qualitatively comparable with the difference of the experimental data. Compared with the experimental squared center of mass energy  $S = 320$  GeV<sup>2</sup>, the value of the  $P_{h\perp}$  is in a reasonable region. The similar situation

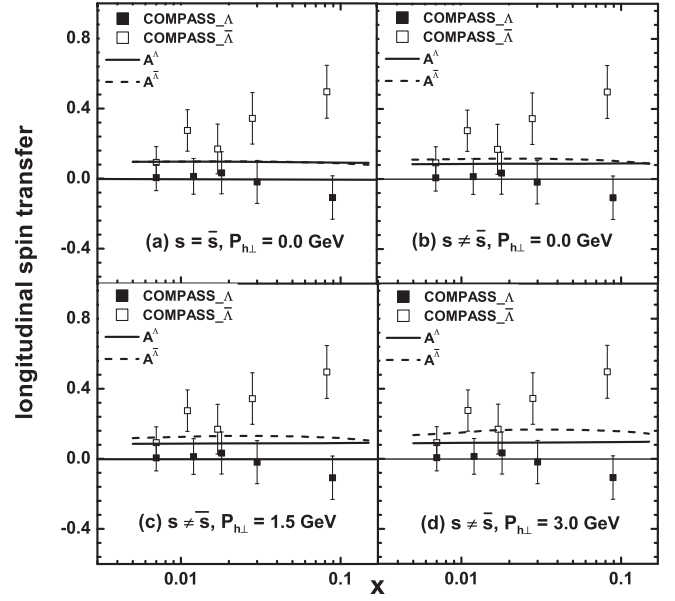


FIG. 2. The results of the  $x$ -dependent longitudinal spin transfer in the polarized charged lepton DIS process for the  $\Lambda$  and  $\bar{\Lambda}$  hyperons. Inputs of the proton strange sea asymmetry and the  $P_{h\perp}$  nonzero values are considered step by step as shown in the subfigures. The data are taken from COMPASS [22].

appears in the  $x_F$ -dependent spin transfer calculations, and we show the results in Figs. 3 and 5.

Combining the first step calculation results with the  $x$ ,  $y$  and  $z$  variable constraints, we can suppose that on the

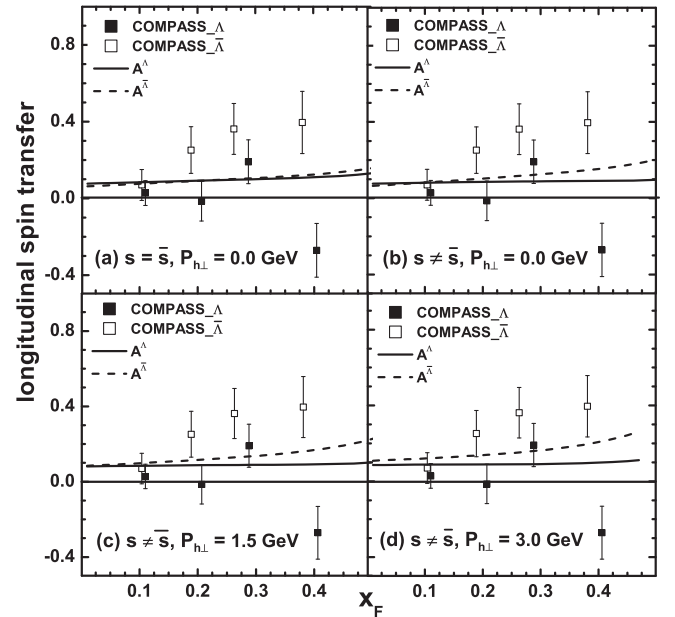


FIG. 3. The results of the  $x_F$ -dependent longitudinal spin transfer in the polarized charged lepton DIS process for the  $\Lambda$  and  $\bar{\Lambda}$  hyperons. Inputs of the proton strange sea asymmetry and the  $P_{h\perp}$  nonzero values are considered step by step as shown in the subfigures. The data are taken from COMPASS [22].

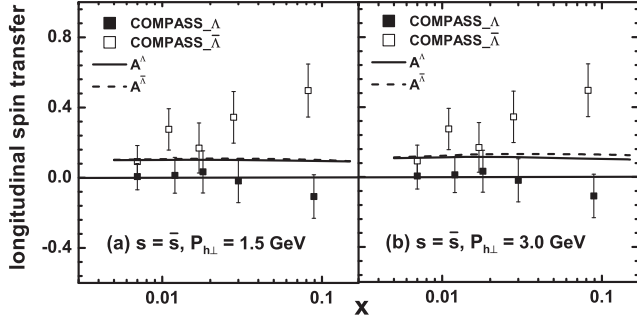


FIG. 4. The results of the  $x$ -dependent longitudinal spin transfer in the polarized charged lepton DIS process for the  $\Lambda$  and  $\bar{\Lambda}$  hyperons. The input of the proton strange sea is symmetry but the  $P_{h\perp}$  is nonzero. The data are taken from COMPASS [22].

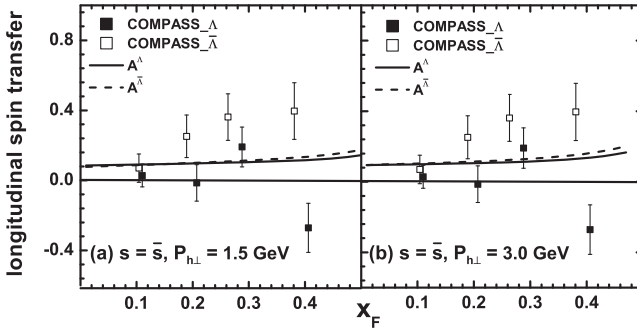


FIG. 5. The results of the  $x_F$ -dependent longitudinal spin transfer in the polarized charged lepton DIS process for the  $\Lambda$  and  $\bar{\Lambda}$  hyperons. The input of the proton strange sea is symmetry but the  $P_{h\perp}$  is nonzero. The data are taken from COMPASS [22].

asymmetric strange sea input basis, the enlarged difference between the  $\Lambda$  and  $\bar{\Lambda}$  longitudinal spin transfers with the increased input value of  $P_{h\perp}$  is in fact from the right shifting  $z$  responsible region.

Figures 4 and 5 show the second step calculation result. It is obvious that without the asymmetric nucleon strange sea input, the influence to the spin transfer difference from the nonzero  $P_{h\perp}$  is non-neglected but still too small.

Comparing these two step discussions, we can reasonably speculate that the large  $z$  region is more sensitive to the asymmetric nucleon strange sea input, and this sensitivity can give better explanations to the experimental data. So we suggest new and precise experimental measurement of the  $\Lambda$  and  $\bar{\Lambda}$  production in the large  $z$  region to give more precise examination of the existence of the nucleon strange sea asymmetry.

## V. SUMMARY

In summary, we studied the quark to the  $\Lambda$  and  $\bar{\Lambda}$  fragmentation properties in the current-fragmentation region by taking various fragmentation processes into account. These processes include the intermediate decay

process and the antiquark fragmentation process, while the strange sea asymmetry in the nucleon is also taken into account. The calculation in the light-cone quark-diquark model shows that the strange sea  $s\bar{s}$  asymmetry gives proper trend to the difference between the  $\Lambda$  and  $\bar{\Lambda}$  longitudinal spin transfers. While considering the nonzero final hadron transverse momentum, our calculation results can explain the COMPASS data reasonably. We interpret the nonzero final hadron transverse momentum as a natural constraint to the final hadron  $z$  range where the longitudinal spin transfer is more sensitive to the strange sea asymmetry. We suggest new and precise experimental measurement of the  $\Lambda$  and  $\bar{\Lambda}$  production in the large  $z$  region to make more precise examination on the nucleon strange sea distributions.

## ACKNOWLEDGMENTS

We would like to thank Tianbo Liu and Lijing Shao for helpful discussions. This work is partially supported by National Natural Science Foundation of China (Grants No. 11035003, No. 11120101004 and No. 11475006) and by the Research Fund for the Doctoral Program of Higher Education (China).

## APPENDIX

Let us first define two Sudakov vectors  $p$  and  $n$  in the light-cone form as

$$p^\mu = (\Lambda, 0, \mathbf{0}_\perp), \quad n^\mu = (0, \Lambda^-, \mathbf{0}_\perp), \quad (\text{A1})$$

where  $\Lambda$  is arbitrary.

Then the nucleon 4-momentum  $P$  and the virtual photon 4-momentum  $q$  in the “ $\gamma^*N$  collinear frames” can be represented in the form of the Sudakov vectors as

$$P^\mu = p^\mu + \frac{1}{2}M^2n^\mu, \\ q^\mu = \frac{Q^2}{2M^2x} \left( 1 - \sqrt{1 + \frac{4M^2x^2}{Q^2}} \right) p^\mu \\ + \frac{Q^2}{4x} \left( 1 + \sqrt{1 + \frac{4M^2x^2}{Q^2}} \right) q^\mu, \quad (\text{A2})$$

where  $M$  is the invariant mass of the nucleon,  $x$  is the Bjoken variable and  $Q^2$  is defined as  $Q^2 = -q^2$ .

We write the 4-momentum of the final hadron  $P_h$  in the  $\gamma^*N$  collinear frame as

$$P_h^\mu = ap^\mu + bn^\mu + P_{h\perp}^\mu, \quad (\text{A3})$$

where  $P_{h\perp}$  is the transverse vector of the final hadron which is perpendicular to the  $p^\mu$  and  $n^\mu$  plat.

The Lorentz invariant variable  $z$  is defined as  $z = P \cdot P_h / P \cdot q$  and for the final hadron it obeys  $P_h^2 = M_h^2$ , where  $M_h$  is the final hadron invariant mass. Using these two



constraints, we can get the values of  $a$  and  $b$ . With two variables,

$$R = \sqrt{1 + \frac{2M^2x}{P \cdot q}},$$

$$R' = \sqrt{1 - \frac{M^2(M_h^2 + P_{h\perp}^2)}{z^2(P \cdot q)^2}}, \quad (\text{A4})$$

$P_h$  can be written as

$$P_h^\mu = \frac{zP \cdot q}{M^2} \left(1 - \frac{R'}{R}\right) P^\mu + z \frac{R'}{R} q^\mu + P_{h\perp}^\mu. \quad (\text{A5})$$

Then the Feynman variable  $x_F$  can be obtained as

$$x_F = \frac{S_{yz}}{M[M^2 + S_y(1-x)]} \left[ \left( M + \frac{S_y}{2M} \right) \times \sqrt{\frac{1 - [4M^2(M_h^2 + P_{h\perp}^2)]}{(S_{yz})^2}} - \sqrt{\frac{S^2 y^2}{4M^2} + S_{xy}} \right]. \quad (\text{A6})$$

- 
- [1] S. J. Brodsky and B.-Q. Ma, *Phys. Lett. B* **381**, 317 (1996).
- [2] A. I. Signal and A. W. Thomas, *Phys. Lett. B* **191**, 205 (1987).
- [3] M. Burkardt and B. Warr, *Phys. Rev. D* **45**, 958 (1992).
- [4] A. Szczurek, H. Holtmann, and J. Speth, *Nucl. Phys.* **A605**, 496 (1996).
- [5] B.-Q. Ma, *Phys. Lett. B* **408**, 387 (1997).
- [6] B.-Q. Ma, I. Schmidt, and J. Soffer, *Phys. Lett. B* **441**, 461 (1998).
- [7] H. R. Christiansen and J. Magnin, *Phys. Lett. B* **445**, 8 (1998).
- [8] W. Melnitchouk and M. Malheiro, *Phys. Lett. B* **451**, 224 (1999).
- [9] B.-Q. Ma, I. Schmidt, J. Soffer, and J.-J. Yang, *Eur. Phys. J. C* **16**, 657 (2000).
- [10] Y. Ding and B.-Q. Ma, *Phys. Lett. B* **590**, 216 (2004).
- [11] J. Alwall and G. Ingelman, *Phys. Rev. D* **70**, 111505 (2004).
- [12] Y. Ding, R.-G. Xu, and B.-Q. Ma, *Phys. Lett. B* **607**, 101 (2005); *Phys. Rev. D* **71**, 094014 (2005).
- [13] P. Gao and B.-Q. Ma, *Eur. Phys. J. C* **44**, 63 (2005); **50**, 603 (2007); *Phys. Rev. D* **77**, 054002 (2008).
- [14] M. Wakamatsu, *Phys. Rev. D* **71**, 057504 (2005).
- [15] J. R. Ellis, A. Kotzinian, D. Naumov, and M. Sapozhnikov, *Eur. Phys. J. C* **52**, 283 (2007).
- [16] F. X. Wei and B. S. Zou, *Phys. Lett. B* **660**, 501 (2008).
- [17] M. Diehl, T. Feldmann, and P. Kroll, *Phys. Rev. D* **77**, 033006 (2008).
- [18] G.-Q. Feng, F.-G. Cao, X.-H. Guo, and A. I. Signal, *Eur. Phys. J. C* **72**, 2250 (2012).
- [19] S. Catani, D. de Florian, G. Rodrigo, and W. Vogelsang, *Phys. Rev. Lett.* **93**, 152003 (2004).
- [20] A. O. Bazarko *et al.* (CCFR Collaboration), *Z. Phys. C* **65**, 189 (1995).
- [21] G. P. Zeller *et al.* (NuTeV Collaboration), *Phys. Rev. Lett.* **88**, 091802 (2002); **90**, 239902(E) (2003).
- [22] M. Alekseev *et al.* (COMPASS Collaboration), *Eur. Phys. J. C* **64**, 171 (2009).
- [23] B.-Q. Ma and J. Soffer, *Phys. Rev. Lett.* **82**, 2250 (1999).
- [24] B.-Q. Ma, I. Schmidt, J. Soffer, and J.-J. Yang, *Phys. Lett. B* **488**, 254 (2000); **489**, 293 (2000); *Phys. Rev. D* **64**, 014017 (2001); **64**, 099901(E) (2001).
- [25] H. L. Lai, J. Huston, S. Kuhlmann, J. Morfin, F. Olness, J. F. Owens, J. Pumplin, and W. K. Tung (CTEQ Collaboration), *Eur. Phys. J. C* **12**, 375 (2000).
- [26] Y. Chi and B.-Q. Ma, *Phys. Lett. B* **726**, 737 (2013).
- [27] R. L. Jaffe, *Phys. Rev. D* **54**, R6581 (1996).
- [28] C. Adolph *et al.* (COMPASS Collaboration), *Eur. Phys. J. C* **73**, 2581 (2013).
- [29] R. Gatto, *Phys. Rev.* **109**, 610 (1958).
- [30] Beringer *et al.* (Particle Data Group), *Phys. Rev. D* **86**, 010001 (2012).
- [31] H. J. Melosh, *Phys. Rev. D* **9**, 1095 (1974); E. Wigner, *Ann. Math.* **40**, 149 (1939); See also, F. Buccella, C. A. Savoy, and P. Sorba, *Lett. Nuovo Cimento* **10**, 455 (1974).
- [32] B.-Q. Ma, *J. Phys. G* **17**, L53 (1991).
- [33] B.-Q. Ma and Q.-R. Zhang, *Z. Phys. C* **58**, 479 (1993).
- [34] B.-Q. Ma, *Phys. Lett. B* **375**, 320 (1996); **380**, 494(E) (1996).
- [35] V. N. Gribov and L. N. Lipatov, *Phys. Lett. B* **37**, 78 (1971).
- [36] V. N. Gribov and L. N. Lipatov, *Yad. Fiz.* **15**, 1218 (1972) [*Sov. J. Nucl. Phys.* **15**, 675 (1972)].
- [37] S. J. Brodsky and B.-Q. Ma, *Phys. Lett. B* **392**, 452 (1997).
- [38] V. Barone, A. Drago, and B.-Q. Ma, *Phys. Rev. C* **62**, 062201 (2000).
- [39] B.-Q. Ma, I. Schmidt, J. Soffer, and J.-J. Yang, *Phys. Rev. D* **62**, 114009 (2000).
- [40] S. J. Brodsky, T. Huang, and G. P. Lepage, *Conf. Proc. C* **810816**, 143 (1981).
- [41] H. J. Weber, *Phys. Rev. D* **49**, 3160 (1994).
- [42] C. Boros, J. T. Londergan, and A. W. Thomas, *Phys. Rev. D* **61**, 014007 (1999).